Available online at www.sciencedirect.com
SCIENCE DIRECT®
Geomorphology 61 (2004) 189–207
GEOMORPHOLOGY
www.elsevier.com/locate/geomorph

Sediment generation and delivery from large historic landslides in the Southern Alps, New Zealand

Oliver Korup[a,*], Mauri J. McSaveney[b], Timothy R.H. Davies[c]

[a] School of Earth Sciences, Victoria University of Wellington, P.O. Box 600, New Zealand
[b] Institute for Geological and Nuclear Sciences, Gracefield Research Centre, Lower Hutt, New Zealand
[c] Natural Resources and Engineering, Lincoln University, Canterbury, New Zealand

Received 20 August 2003; received in revised form 13 December 2003; accepted 15 December 2003

Available online 5 February 2004

Abstract

There is much variability of sediment yield in mountain river systems because it is influenced by both periodic (e.g., snowmelt, monsoonal circulation) and episodic (high-intensity rainstorms, earthquakes) controls. In the Southern Alps of New Zealand, landslides are dominant mechanisms of conveying large amounts of debris to river channels. This paper attempts to quantify catastrophic modes of sediment delivery by presenting three recent examples of large landslides on the western slopes of the Southern Alps. A combination of ground surveys, DEM-based volume calculations, and air photo interpretation attributes immediate postfailure sediment yields in excess of 70,000 t km^{-2} a^{-1} in the short term. Such landslide-derived sediment pulses pose significant hazards to downstream settlements and infrastructure on alluvial fans, where they cause massive aggradation, increased flooding frequency, and large-scale channel avulsion. In addition to intramontane valley floor obliteration or channel metamorphosis, these geomorphic impacts may thus occur far beyond the initial locations of slope failure. These catastrophic off-site effects involve apparent net sediment delivery rates in the order of 10^5–10^6 m^3 a^{-1}. The accurate quantification of the relative contribution of debris from the disturbing landslide to overall sediment flux is extremely difficult. Nonetheless are quantitative estimates of landslide-derived sediment production and delivery important data to develop a more comprehensive understanding of the variability in alpine sediment flux. Such data are essential not only for use in hydraulic engineering or catchment management, but also in gauging potential future impacts from rainstorm- and earthquake-induced landsliding in the Southern Alps.

Keywords: Sediment yield; Sediment delivery; High mountain geomorphology; Landslide dam; Avulsion; River metamorphosis

1. Introduction

The assessment of fluvial sediment yields in mountain drainage basins is an important challenge in geomorphology. Alpine terrain limits effective sampling strategies and poses technical difficulties in measuring the bed-load component of total yield in gravel-bed rivers and torrents (Carson and Griffiths, 1987). Alpine sediment yields exhibit a high natural variability, the signal of which may bear significant imprints of anthropogenic activity (e.g., Alvera and García-Ruiz, 2000). Instrumental observations from direct measurements usually cover short periods and

* Corresponding author. Present address: WSL Swiss Federal Institute for Snow and Avalanche Research SLF, Flüelastr. 11, Davos CH-7260, Switzerland. Tel.: +41-81-417-0354; fax: +41-81-417-0110.
E-mail address: korup@slf.ch (O. Korup).

0169-555X/$ - see front matter © 2004 Elsevier B.V. All rights reserved.
doi:10.1016/j.geomorph.2004.01.001

often account only for the suspended fraction of sediment yield (Walling and Webb, 1996). In contrast, long-term rates derived from off-site evidence such as lake sediments may contain systematic or censoring-based errors, which can usually be allowed for (Hicks et al., 1990; Evans, 1997; Evans and Church, 2000; Schiefer et al., 2001).

In tectonically active mountain belts such as the collisional orogen of the Southern Alps, New Zealand, frequent landsliding and fluvial dissection are the main agents of denudation. Close geomorphic coupling of hillslope and valley floor systems often favours instantaneous and spatially discrete, i.e., point source sediment delivery to the drainage network (Beschta, 1983; Hovius et al., 1997). This study recognises the lack of quantitative work of sediment budgets related to large landslides. Its general objective is to quantitatively investigate to what degree fluvial sediment yield is altered by both instantaneous and chronic delivery of large ($>10^6$ m^3) amounts of landslide debris. We specifically attempt to estimate the volume of material supplied by large historic landslides in ungauged alpine catchments. By complementing the documented postfailure morphodynamic histories for each respective site, we aim to infer average process rates for regional comparison.

2. Previous work on landslide sediment yields

Landslide-related research rarely addresses the indirect effects of landslides on mountain river channel/valley floor geomorphology and sediment yields (e.g., Miller and Benda, 2000). Large ($>10^6$ m^3) landslides may not only contribute significant amounts of debris to river channels, but also delay or partially impede the delivery by forming temporary or quasipermanent impoundments (Costa and Schuster, 1988). Such temporary sediment retention may lead to extreme geomorphic impacts, as illustrated by the formation and failure of the 1985 earthquake-triggered Bairaman landslide dam in the Nakanai Mountains of Papua New Guinea (King et al., 1989). There, an earthquake-triggered landslide involving some 180×10^6 m^3 of debris created a 200-m-high dam, which was artificially breached. The resulting large hyperconcentrated outburst flood more or less instantaneously supplied some 64×10^6 m^3 of sediment to the Bairaman River for a downstream length of 39 km (Schuster, 2000). The Ama Dablam Rock Avalanche created a landslide dam in the Imja Khola of the Nepal Himalaya in 1979. Breaching of the dam initiated a debris flow that travelled for 20 km downstream, causing valley floor aggradation of 3 m on the average (Selby, 1988, 1993). Fort (1987) described 450-year-old catastrophic debris flows in the Pokhara valley of Central Nepal that had blocked the Seti River; postbreach incision caused a long-term shift in fluvial debris transport, with an annual contribution of landslide-derived sediment in the order of 4×10^6 m^3, a specific sediment yield of nearly 3100 m^3 km^{-2} a^{-1}. In contrast, within 20 min, the 1993 Sesa complex debris slump flow in the Valcamonica, Italian Alps, delivered $\sim 1.6 \times 10^6$ m^3 of sediment to a 7-km reach of Grigna Creek, without causing obvious stream blockage (Crosta, 2001).

Detailed short-term quantitative studies of the erosion of landslide deposits are rare. Ohmori (1992) examined the fluvial dissection of the Ontake debris avalanche, Japan, and provided averaged short-term rates of debris entrainment and evacuation. Sutherland et al. (2002) made detailed measurements of the gradual downstream propagation of a sediment wave following a landslide dam break in a gravel channel. Such case studies are complemented by work on catchment-scale medium-term sediment flux following episodes of coseismic landsliding (e.g., Pearce and Watson, 1986). Nonetheless, single medium to small-scale slope failures can also affect long-term rates of alpine fluvial sediment yields. Ries (2000) described a small (9000 m^3) landslide in the Surma Khola of the High Mountain region of the Central Nepal Himalaya, which during 3 days following failure increased total suspended basin yield to 4 t ha^{-1}, i.e., twice the annual sediment delivery.

In recent years, regional-scale studies have used landslide inventories in attempts to assess the cumulative effects of slope failure on catchment- and regional-scale sediment yields on a decadal scale (e.g., Hovius et al., 1997, 2000). Even in active tectonic environments along the Pacific Rim, upland sediment yields are subject to considerable variation. Martin et al. (2002), for example, have examined sediment production by shallow landsliding in the Queen Charlotte Islands, British Columbia. They

have estimated specific sediment yields of ~ 180 t km^{-2} a^{-1}, equalling a denudation rate of 0.10 mm a^{-1}. These values rank among the maximum rates derived for the Pacific Northwest and coastal British Columbia. Available data for long-term landslide-derived sediment yields from the western slopes of the Southern Alps, New Zealand, exceed those rates by two orders of magnitude (~ 10^4 t km^{-2} a^{-1}; Hovius et al., 1997) and correspond with measurements of fluvial suspended sediment yields (Griffiths, 1979; Hicks et al., 1996).

3. Geomorphic setting of the western Southern Alps

The Southern Alps are the geomorphic expression of an active oblique continent–continent collision of the Indo-Australian and Pacific Plates. This major neotectonic boundary is defined by the largely linear trace of the Alpine Fault. Hanging wall exhumation of metamorphic schist of the Haast Group implies that rapid uplift (up to 10 mm a^{-1}; Norris and Cooper, 2000) has produced an asymmetric orogen steeply emerging to the SE of the dextral transpressional fault (Fig. 1).

Due to its oceanic climate, New Zealand receives a high influx of moisture-laden air conveyed by dominantly northwesterly airflow, to which the roughly NE-striking Southern Alps form a significant barrier with a total relief of nearly 3700 m. Orographic precipitation is extremely high and may attain 14,000 mm a^{-1} near the Main Divide (Henderson and Thompson, 1999). Accordingly, the densely forested western flanks of the Southern Alps exhibit a high degree of dissection by both landsliding and fluvial erosion (Whitehouse, 1988). These dominant erosional processes have produced serrated ridges and steep rectilinear slopes. Short high-gradient flood-prone river systems drain into the Tasman Sea via a narrow coastal footwall piedmont covered by lateral moraine ridges and thick fluvioglacial outwash. Although ~10% of alpine catchments remain glaciated in some headwaters, most of the erosional landscape has been significantly modified since the retreat of lowland glaciers some 14,000 years ago (Suggate, 1990).

Cyclonic high-intensity rainstorms trigger numerous small shallow landslides of the rapid debris slide and debris flow type (Cruden and Varnes, 1996), which strip hillslopes mainly of colluvium and vegetation mats. Earthquake shaking, gravitational stress (especially along planes of schistosity), and debuttressing following recent deglaciation are important conditioning factors for large (>10^6 m^3) deep-seated bedrock landsliding (Whitehouse, 1988; Korup and Crozier, 2002). These slope failures chiefly comprise complex rotational slides/flows and rock-block slides, which have in many places caused temporary blockage or occlusion of alpine river systems (Korup, 2003).

The magnitude and frequency of landslide-derived sediment delivery from the mountain belt to the adjacent foreland is of critical importance to the safety of local settlements and infrastructure, which are primarily located on the alluvial fans of major alpine rivers (Hamblett, 1968; Hancox et al., 1999). In the following, three examples of recent major landslides in the western Southern Alps are presented and their role in catchment sediment flux is investigated.

4. Landslide-related sediment production and delivery, Southern Alps

4.1. Methodology

To estimate the volumes of landslide-related sediment production, we conducted an initial literature review on the case studies. Air photos at nominal scales ~ 1:50,000 taken between 1937 and 2002 were inspected during a regional reconnaissance and used to ascertain temporal markers for sediment delivery (Korup, 2003). A georeferenced 25-m grid Digital Elevation Model (DEM; Land Information New Zealand, 2000) served as a platform for cut-and-fill calculations based on prelandslide and post-landslide surfaces. The underlying assumption for this method was that we could sufficiently reconstruct local degradation and aggradation by joining contours of identified geomorphic surfaces via straight lines, respectively. These lines were repeatedly digitised onto the DEM and used to construct surfaces, which were subsequently subtracted from the original (prefailures) surface to obtain the respective volumes for each time slice. As a means of ground truthing, we conducted and

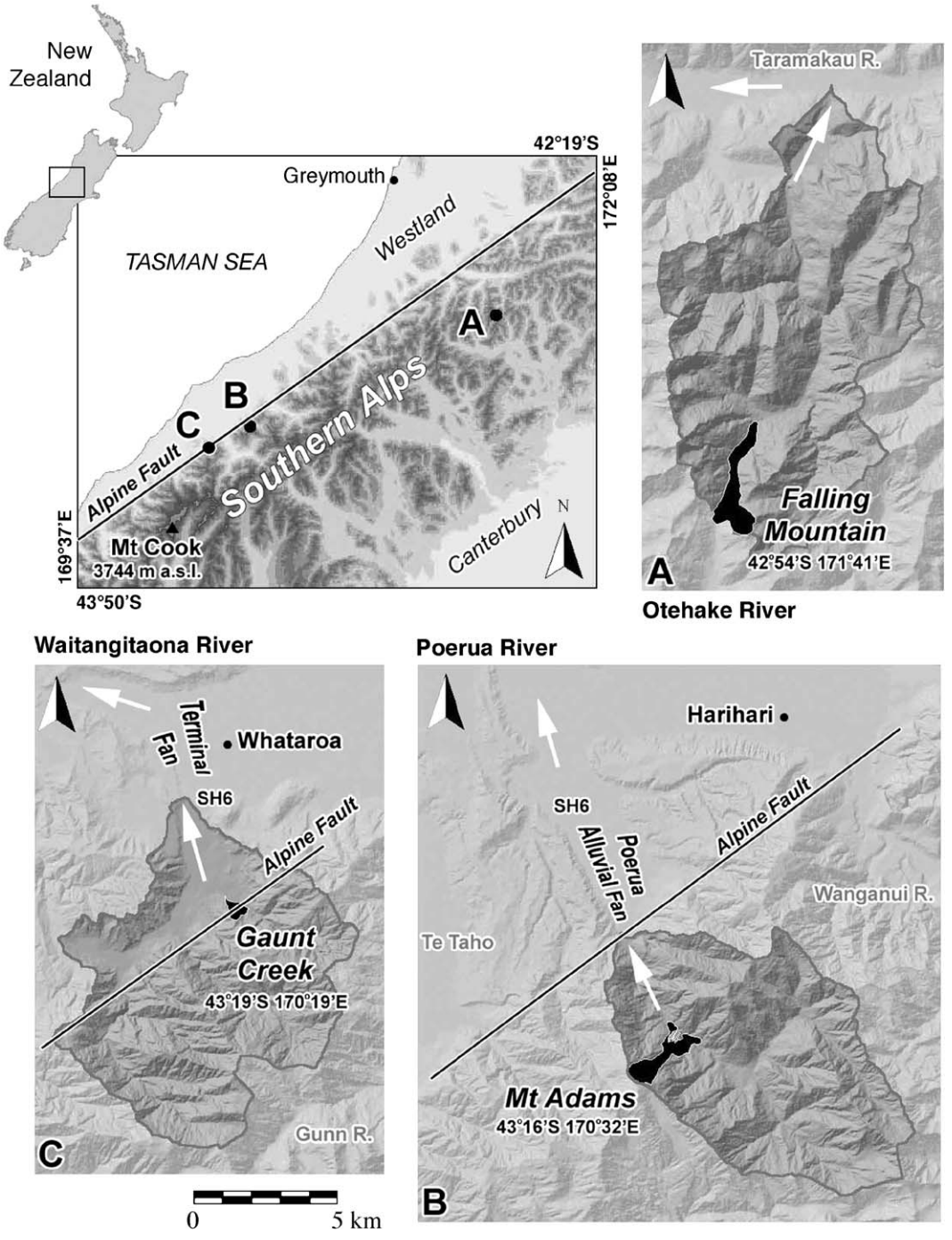

Fig. 1. Location map of Westland and shaded relief maps of the landslide study sites. Catchment areas are shaded dark grey, black areas denote extent of historic landslides, and white arrows mark general drainage direction. (A) Falling Mountain, Otehake River; (B) Mt. Adams, Poerua River; (C) Gaunt Creek, Waitangitaona River. State Highway 6 (SH6). Scale bar applies to catchment maps only; inset coordinates for Panels A–C refer to respective headscarp locations of landslides.

compiled several ground cross-sectional surveys at selected river reaches with an Electronic Distance Meter (EDM) at subcentimetre accuracy. Locations of further geomorphic evidence of historic aggradation such as cut-and-fill terraces, exhumed tree stumps, and exposures of buried soil horizons (Korup, 2003) were surveyed with EDM and a handheld 12-channel GPS receiver at ± 2 m horizontal resolution and a 1:50,000 mapping scale. Particle size in selected river reaches was measured with a calliper and tape and used to calculate trapping efficiency following the method of Griffiths and McSaveney (1986).

4.2. Falling Mountain, Otehake River, Central Westland

4.2.1. Failure history

Instantaneous and catastrophic slope failure may seriously alter sediment transport rates in alpine river systems. A spectacular example is the Falling Mountain rock avalanche (Fig. 1A), which descended from the peak of Falling Mountain and formed Taruahuna Pass (1252 m a.s.l.) on the Main Divide of the New Zealand Southern Alps during the $M_s = 6.9$ Arthur's Pass earthquake in 1929. Catastrophic mass move-

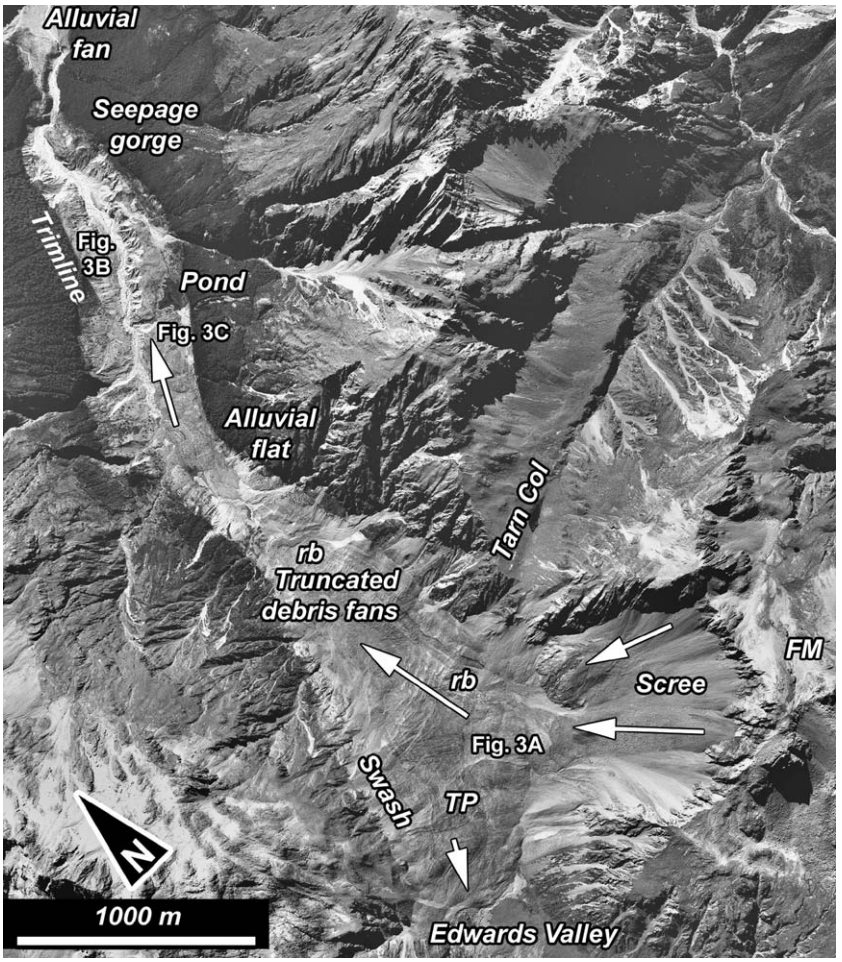

Fig. 2. Air photograph of the major rock avalanche that initiated from Falling Mountain (FM) during the 1929 Arthur's Pass earthquake. The landslide deposit has formed Taruahuna Pass (TP, 1252 m a.s.l.) on the Main Divide of the Southern Alps. Note transverse furrows and remnant bedding (rb) of greywacke–argillite stratigraphy on deposit surface. White arrows depict major directions of flow. Image courtesy of Land Information New Zealand (SN8090/H4, Crown Copyright Reserved).

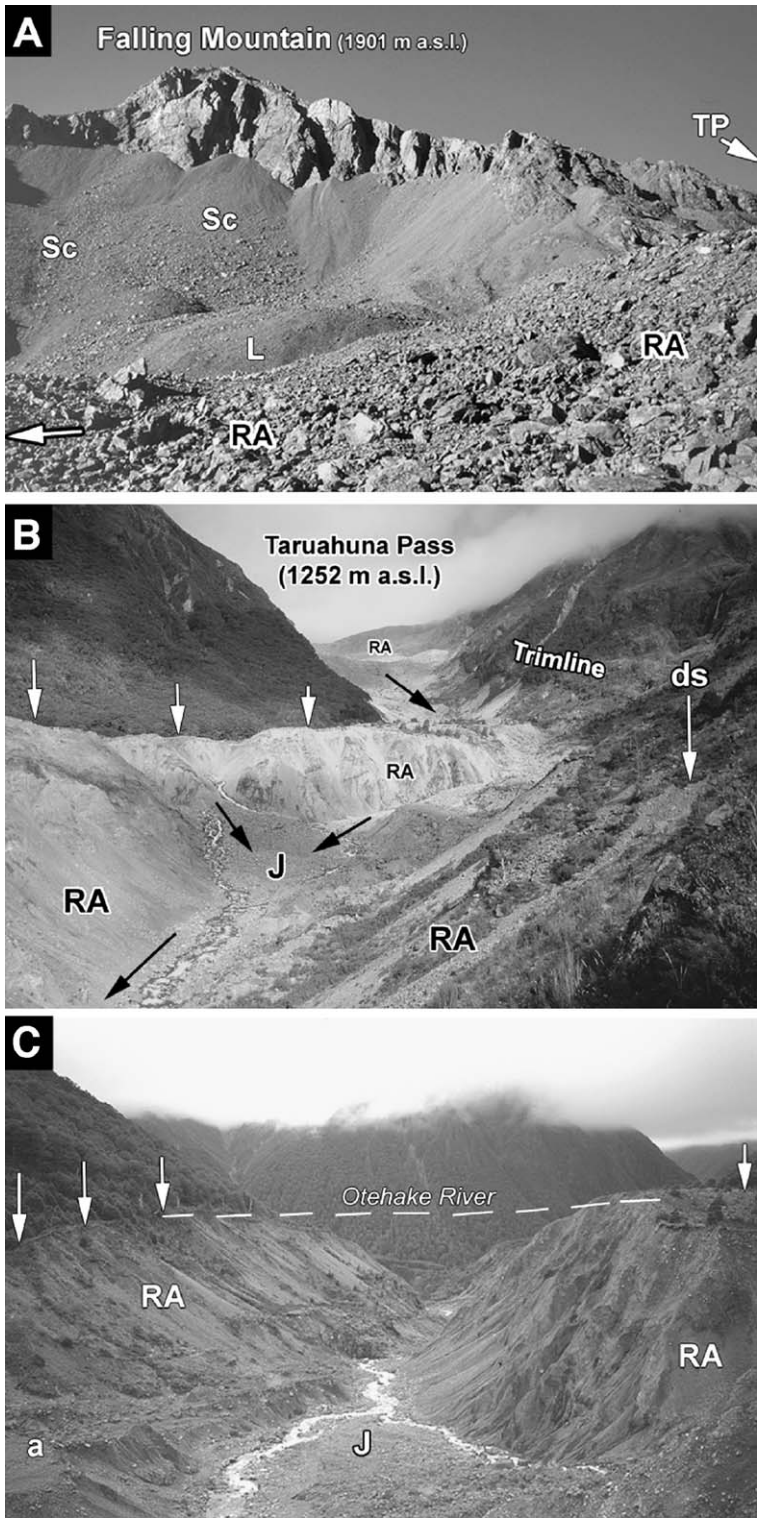
A
Falling Mountain (1901 m a.s.l.)
TP
Sc
Sc
L
RA
RA
B
Taruahuna Pass
(1252 m a.s.l.)
RA
Trimline
ds
RA
J
RA
RA
C
Otehake River
RA
RA
a
J

ment of some ~ 55×10^6 m^3 was most likely triggered by topographic amplification of ground shaking of jointed and indurated greywacke and argillite bedrock. Slope failure commenced as continuous rockfall and deteriorated into a fast-moving rock avalanche that swashed up the opposite valleyside for some 60 m, and raced down the West Branch of the Otehake River for nearly 4.5 km (McSaveney et al., 2000), covering an area of 2.5 km^2 (Fig. 2).

A former bedrock gorge was obliterated by burial up to 80–100 m beneath a deposit of highly disrupted, poorly sorted, and very angular greywacke and argillite debris (Fig. 3). Despite its size, the landslide did not cause any major river blockage with the exception of ponding minor tributaries. This is largely due to its initiation on the Main Divide and channelised downvalley motion.

4.2.2. Postfailure morphodynamics

Nearly 70 years after the event, most of the upper rock avalanche deposit remains in situ below the main scarp, forming hummocky furrowed debris mounds and perched swash marks. With the exception of localised patches of lichen, grass, and a variety of plant species, the deposit is largely unvegetated at subalpine elevations. The 0.65-km^2 headscarp at the NW flank of Falling Mountain is mantled with massive talus ramparts (Fig. 3A). In many locations, the deposit surface exhibits a characteristic jigsaw particle texture (Hewitt, 1999), openwork angular boulder piles, pronounced flow structures like furrows and swales (Fig. 2), as well as remnant lithologic stratigraphy. Parts of the deposit surface have been modified by breakdown of argillite via wetting and drying, and slope smoothing via snow creep. In the midreach, the deposit has been subject to reworking by debris flows issuing from steep tributary ravines, which have added further material to the rock avalanche surface in levee-covered fans and lobes.

In the downstream reaches, the main channel system has reestablished by the formation of a bifurcated and up to ~ 80-m-deep spring-seepage gorge (Fig. 3B and C). Headward retreat has dissected the fine gravely and sandy subsurface distal deposit of the rock avalanche, affecting some 10% of the total landslide area. An intricate system of cut-and-fill debris terraces is preserved in the upper gorge, where-

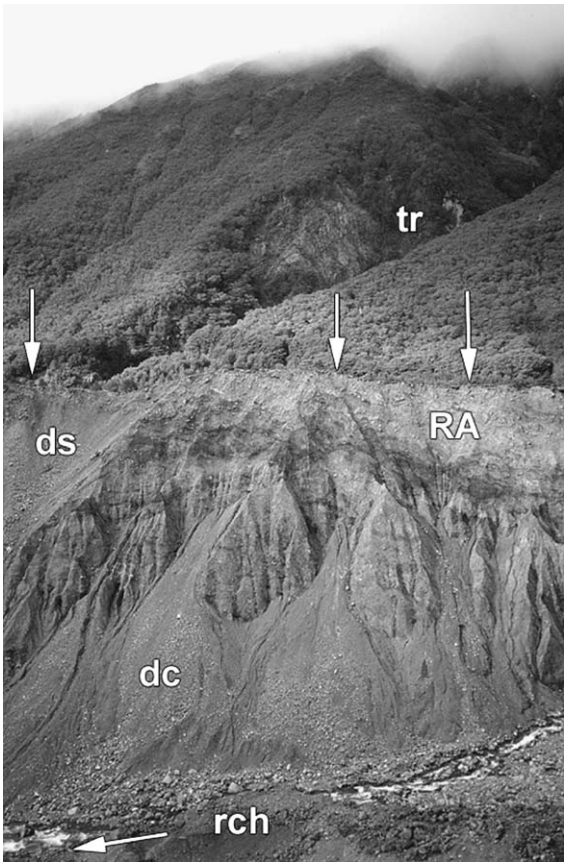

Fig. 4. Detail of ~ 80-m-high right-bank gorge wall incised into Falling Mountain rock avalanche deposit (white arrows show deposit surface). Tributary ravine (tr); secondary debris slide (ds); debris flow cone built from reworked landslide deposit (dc); reexhumed channel (rch). Note the undulating stratification in the rock avalanche deposit.

Fig. 3. Ground views of the 1929 Falling Mountain rock avalanche. (A) SE view of the headscarp area; Taruahuna Pass (TP, arrow to the right of picture); scree cones (Sc) and ramparts mantling the detachment zone; L = debris lobes with superficial reworking by debris flow; rock avalanche (RA) deposit; arrow on left denotes major flow direction of rock avalanche. (B) Upstream view of runout track; white vertical arrows denote vegetation trimlines and deposit surface; black arrows show major direction of flow; J = confluence of reexhumed seepage-fed streams; ds = erosion of deposit surface through secondary debris slide. (C) Downstream view of steep-walled ~ 80-m deep gorge in rock avalanche debris, formed by headward erosion of seepage-fed streams emerging from the deposit interior; (a) inset degradation debris terrace; dashed white line depicts interpolated deposit surface.

as localised backfilling of swales is evident in the deposit surface by fluvially reworked rock avalanche material. The gorge sidewalls are subject to active debris slide, fall, and flow (Fig. 4).

The downstream extent of the landslide deposit is marked by a vegetation trimline, which is tongue-shaped in planform and grades into a small (0.12 km^2) alluvial fan (Fig. 2). Any evidence of further aggradation is either absent or lost in the inaccessible downstream bedrock gorge sections of the Otehake River.

4.2.3. Sediment contribution

On both valleysides, trimlines bound perched and upwardly convex landslide deposits, remnants of the original extent of the rock avalanche surface. Thus, estimates of the fluvially excavated volume of the deposit provide information on the long-term sediment discharge. The amount of eroded landslide debris was estimated from air photo-based mapping and volume calculations with the 25-m DEM. Contour lines have been extrapolated across the shingle gorge sidewalls, assuming a horizontal deposit surface (Fig. 3C). We have used this simplification despite the possibility that the thicker rock avalanche material in the gorge kept flowing, after the thinner material on the valleysides became stranded, to produce a more concave cross profile.

Based on plane projections over the distal deposit scour, an average sediment yield of 35,200 $\pm$ 2300 t km^{-2} a^{-1} ($\pm$ 1 standard error) has been calculated for a period of 62 years.

4.3. Mt. Adams, Poerua River, South Westland

4.3.1. Failure history

On 6 October 1999, a large rock avalanche fell from the ridgeline at Mt. Adams above the lower Poerua River gorges (Fig. 1B). The failure involved some 10–15 $\times$ 10^6 m^3 of schist and colluvium, occurred without any obvious trigger, and formed an 80–100-m-high dam in the gorge (Hancox et al., 1999; Fig. 5).

The resulting lake overtopped the dam 2 days after the landslide fell. The dam lasted 6 days after overtopping and failed during a minor fresh, which caused an outburst flood with peak discharge in the order of 1000–3000 m^3 s^{-1} (Hancox et al., 1999). The rapid downstream sluicing of landslide debris resulted in massive fanhead aggradation at the mountain range front. More than 3 years after the event, downstream deposition continues and has initiated a major avulsion sequence along a former inactive channel, engulf-

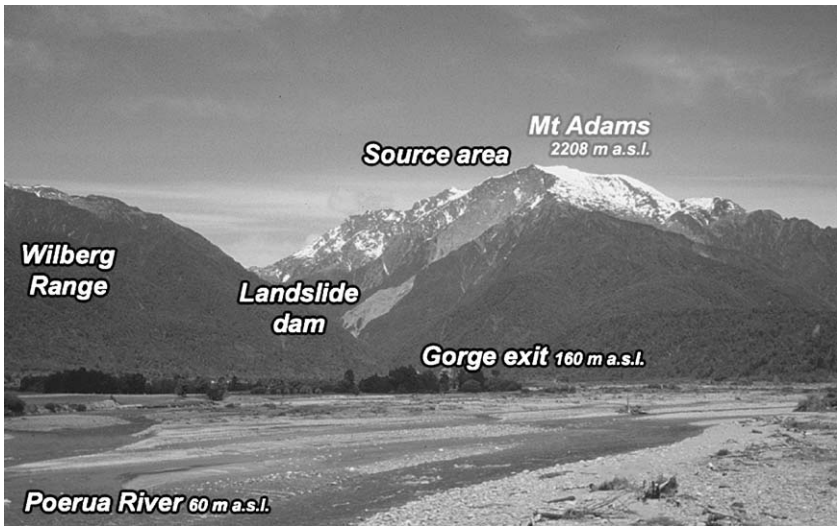

Fig. 5. View S from the South Westland foreland towards 1999 Mt. Adams rock avalanche and landslide dam remnant in the Poerua River gorge (distance ~ 7 km, cf. Fig. 6). This fault-bounded mountain–foreland setting is characteristic for South Westland and bears a high potential for adverse long-range effects of large landslides.

ing some 0.9 km^2 of mainly forested floodplain and farmland.

4.3.2. Postfailure sediment flux

A 25-m grid DEM predating the event has been used to estimate the amount of sediment delivery and downstream aggradation in the lower Poerua River gorges and on the alluvial fan at the mountain–foreland transition. Recent air photography obtained on January 2001 and 2002 has been compared with earlier images dating back to 1984 to trace the extent of geomorphic changes related to the landslide dam (Fig. 6). The cascading nature of postfailure aggradation is clearly evident in newly formed intramontane flats bounded by distinctive vegetation trimlines, which have been graphically superimposed onto the DEM. This process has been supported by use of a stereoscope and repeated several times as to minimise errors of distortion inherent to air photos. The intersection points of mapped deposit margins with the 20-m contour lines were used to extrapolate aggradation surfaces and subsequently calculate infill volumes by using standard GIS-based cut-and-fill algorithms. The modelled areas of net sediment gain from various scenarios were then calibrated to match the mapped deposits as closely as possible.

In addition, 38 repeat cross-sectional surveys of the Poerua alluvial fan have been conducted during several campaigns to trace temporal changes in bed elevation downstream of the gorge (Fig. 7). The channel area of each cross-section was multiplied with the mean distance between sections to obtain volumetric estimates of net sediment flux.

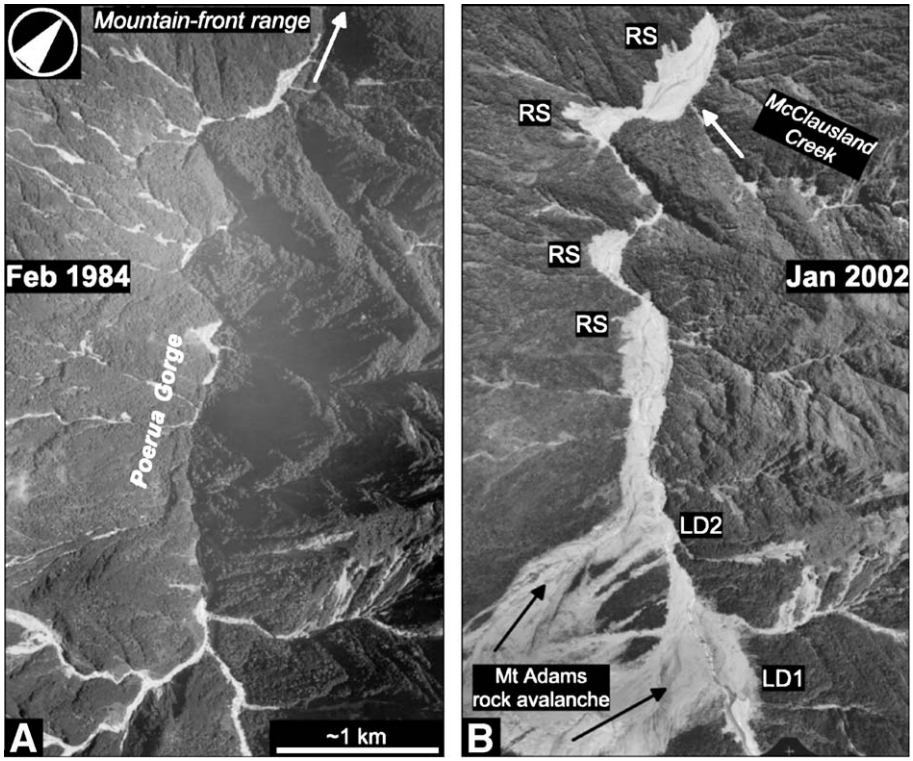

Fig. 6. Sequential air photography of massive aggradation on the lower Poerua River following failure of the 1999 Mt. Adams rock avalanche dam. (A) Channel morphology in February 1984 is dominated by bedrock gorges; (B) Landslide emplacement and dam failure in late 1999 has created a sequence of cascading intramontane alluvial flats, which have effectively backfilled the gorges, transforming an erosional into a depositional environment: landslide dam remnants (LD1, 2); aggradation-induced riparian slips (RS). Images courtesy of Land Information New Zealand and Department of Natural Resources and Engineering, Lincoln University (Panel A: SNC8340/D24; Panel B: SN12690B/A11).

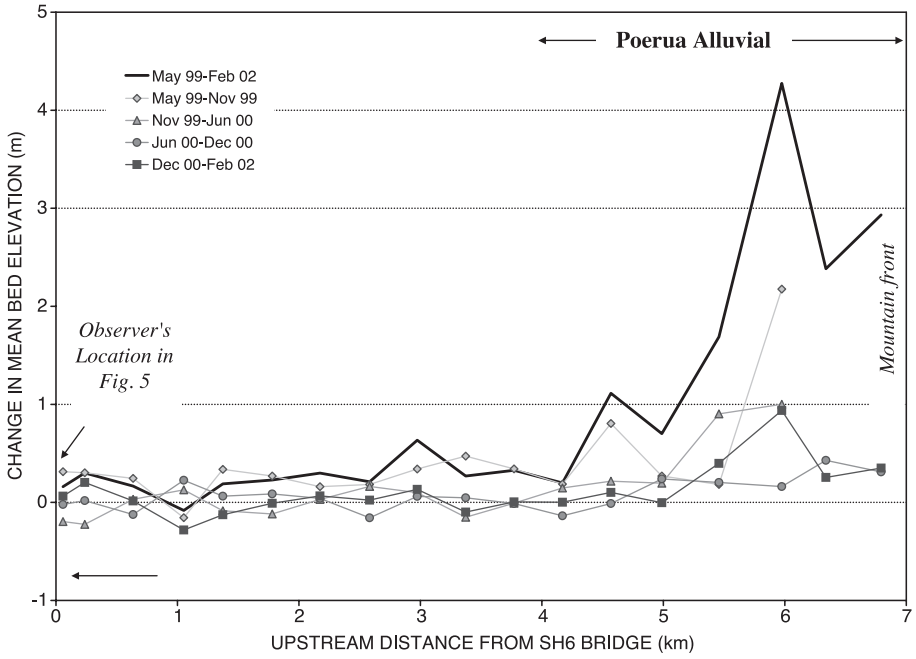

Fig. 7. Sequence of changes in relative elevation of the Poerua River alluvial fan following the Mt. Adams rock avalanche dam failure. Flow is from right to left. Fanhead aggradation exceeded 2 m approximately 1 month after the dam failure; short-term aggradation peaked at >4 m in less than 3 years after the event.

Conservative scenarios from GIS-modelling suggest that $\sim 5.5 \times 10^6$ m^3 have been deposited in the lower Poerua River gorges since the failure of the landslide dam. Temporary sediment storage in three major intramontane flats covers 0.3 km^2 in total and results from the infilling of bedrock gorges with an average deposit thickness of ~ 20 m. Assuming a contributing catchment area of ~ 59 km^2 just above the lowest gorge, the resulting average specific sediment yield at this location would approximate $\sim 75{,}700 \pm 4600$ t km^{-2} a^{-1}. It is not feasible to isolate the relative contribution of landslide dam derived debris because the aggradation process may have favoured the temporary trapping of sediment from sources further upstream as well. Furthermore, there is the possibility that significant amounts of debris in the gorge may have been redeposited by nonfluvial processes such as debris/hyperconcentrated flows or gravity collapse during early stages of the dam-breach sequence. Subsequent sluicing of rock avalanche debris from the lower transport slopes by reestablished mountain torrents as well as secondary landsliding triggered by fluvial scour has subsequently added sediment to the channel.

Field visits in early 2002 revealed that avulsion channel establishment was still in an early stage, incorporating braided, locally cascading flow of several channels and chutes through remnant forest and buried undergrowth. At various upper fan locations, exposures of recently buried soils indicate 2 m of recent aggradation some 2 km downstream from the gorge. The exhumation of buried soil surfaces under the presently aggrading area indicates that the present event had a number of predecessors. By January 2001, fanhead aggradation had sent initial debris splays onto a blazed farm track near the 150-m contour line, thus requiring a minimum aggradation of ~ 15 m at the gorge outlet. This is consistent with recent survey data observations of ongoing tributary backfilling at Rata Creek at the mountain front range, and burial of a former 10-m-high aggradation terrace, which had been ^{14}C-dated to 295 ± 55 BP (NZ4630, D. Chambers, personal communication, 2002).

4.4. Gaunt Creek, Waitangitaona River, South Westland

4.4.1. Failure history

Gaunt Creek drains a small tributary basin ($A = 9.1$ km^2) of the Waitangitaona River, South Westland, in the western mountain front range of the Southern Alps (Fig. 1C). Truncation of the catchment by the Alpine Fault has resulted in tectonic weakening and hydrothermal alteration of Haast Group schist bedrock, forming a fault zone of highly erodible cataclasite and mylonite. Historic slope instability at Gaunt Creek, presumably triggered by fluvial undercutting, was first reported on the mountain front in 1918 (Griffiths and McSaveney, 1986). Since then, a 0.34-km^2 section of the mountain front locally known as "Gaunt Creek Slip" (Fig. 8) has been chronically unstable, promoting high-frequency mass movements induced by both rainstorms and fluvial debuttressing.

Progressive landslide sediment delivery of ~ 7.7×10^6 m^3 between 1918 and 1965 (Hamblett, 1968) initiated pulses of massive aggradation on the fault-bounded low-angle fan of Gaunt Creek. The buildup of debris had started to overwhelm the fan channel capacity by the 1940s, causing burial of floodplain forests on elevated outwash terraces. By 1967, the sediment wave had propagated to the mountain-fringe fan of the Waitangitaona River, about 3 km further downstream, culminating in a large-scale channel avulsion (Fig. 8).

Following abandonment of the old channel, the Waitangitaona River gradually formed a new active terminal fan–delta complex across some 3.7 km^2 of swamp and farmland, and commenced to infill Lake Wahapo in the Okarito River catchment.

4.4.2. Landslide signals in sediment yield

The detailed geomorphic response sequence of the avulsion event has been described elsewhere (Korup,

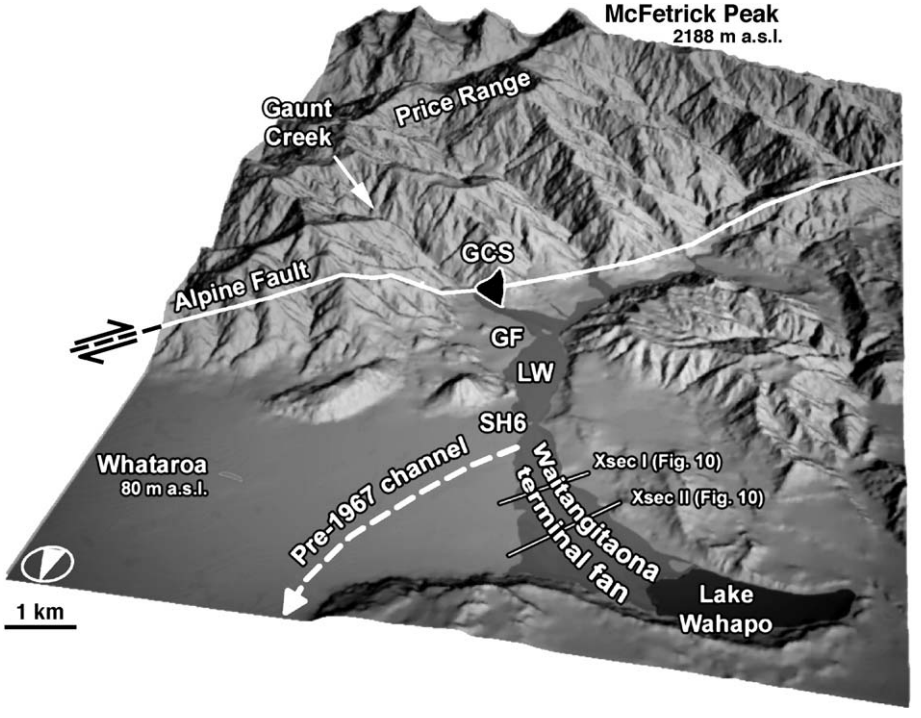

Fig. 8. Large-scale landslide-driven channel avulsion on the Waitangitaona River. Chronic instability in mylonitic schist of the Alpine Fault zone ("Gaunt Creek Slip", GCS) has led to massive aggradation on Gaunt Creek Fan (GF), lower Waitangitaona River (LW), and triggered a major channel avulsion at State Highway 6 (SH6) bridge in 1967. Reactivation of distal portions of Waitangitaona terminal fan has caused burial of farmland and increase of discharge into Lake Wahapo.

2003) and is not discussed here in further detail. In contrast to the relative remoteness of Falling Mountain, the Waitangitaona River lies in the vicinity of the major traffic conduit of State Highway 6 (SH6), as well as extensive farmland and housing. As with numerous other places in South Westland, monitoring of the sediment load on the alluvial fan at the mountain front is of high relevance for the structural integrity of both the SH6 bridge and the stopbanks fringing the active fan head (Davies and McSaveney, 2000).

Dynamics of sediment yield have been reconstructed for both the Gaunt Creek and Waitangitaona River terminal fans. Air photo coverage of these areas allowed the temporal bracketing of the formation of numerous conspicuous aggradation and degradation terraces on Gaunt Creek Fan in 11 time slices between 1948 and 1987. Cobble nests and perched grassed remnants of aggradation surfaces in exhumed in situ tree cohorts have provided further evidence of minimum burial depths (Fig. 9; Korup, 2003).

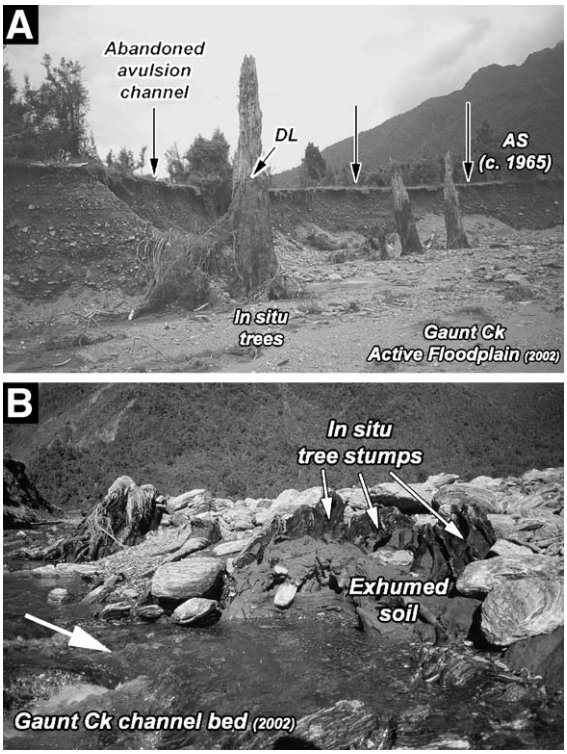

Fig. 9. Indicators of recent aggradation/degradation cycles on Gaunt Creek, Waitangitaona River catchment. (A) Active terrace scarp developed in ~1965 fan aggradation surface (AS, vertical arrows). Deterioration level of wood (DL) on in situ stand of excavated trees in active channel bed of Gaunt Creek accords with terrace tread and implies historical burial. Average scarp height is ~6 m. (B) Detail of exhumed forest soil with in situ tree stumps on left bank of cobble-dominated channel bed. Height of channel bank is ~0.8 m.

Cross-sectional surveys were done by GPS and EDM and coupled with the 25-m DEM for calculation of net losses in sediment volume for each terrace level. Rates of sediment contribution were obtained by dividing the missing volumes for each surface level by the approximate time interval between its formation and dissection as evident from air photography. The resulting sediment budget has been augmented with recent observations of rainstorm-driven bank erosion of fan terraces in the summer 2001/2002 (Table 1).

Based on extrapolation of surfaces from aggradation terraces and cobbles nests in tree cohorts, the Gaunt Creek fan shows a net loss of $\sim 3.6 \times 10^6$ m^3 between 1965 and 2001, which translates to a specific sediment yield of 26,800 t km^{-2} a^{-1} at Gaunt Creek confluence, based on a fan trapping efficiency $E_t = 0.61$. This is more than twice the yield estimated for the Waitangitaona River at SH6 (Griffiths and McSaveney, 1986). Although particle size analysis of fan material in 2001 resulted in values as low as $E_t = 0.44$ (Table 1), we regard the higher value as more realistic during periods of pronounced aggradation. Consequently, maximum relative errors for these estimates amount up to 30% (Table 1).

Repeat cross-sectional survey data from 1982, 1992, and 2001 provided by the West Coast Regional Council, Greymouth (M. Shearer, personal communication, 2001), have been employed to estimate the sediment dynamics on the Waitangitaona terminal fan downstream of the SH6 bridge (Fig. 10).

Griffiths and McSaveney (1986) have employed a simple equation of trapping efficiency for reservoirs to estimate the total specific sediment yield of the Waitangitaona River. Because their calculations were dependent on the particle size differences between sediment source and sink location, i.e., Gaunt Creek Slip and Lake Wahapo fan-toe delta,

Table 1
Sediment budgets for the Gaunt Creek and Waitangitaona River terminal fans

(a) Gaunt Creek fan

Input (m^3)	Input rate (m^3 a^{-1})	Specific sediment yield (t km^{-2} a^{-1})	Relative error (%)[a]	Trap efficiency	Source
1918–1965					
7.7×10^6	164,000	32,800	–	–	Hamblett (1968)
Output (m^3)	Output rate (m^3 a^{-1})	Specific sediment yield (t km^{-2} a^{-1})	Relative error (%)[a]	Trap efficiency	Source
1965–2001					
3.58×10^6	99,500	16,300	12.7		This Study
		26,800		0.61	This Study
		37,000		0.44	This Study

(b) Waitangitaona terminal fan

Input (m^3)	Input rate (m^3 a^{-1})	Specific sediment yield (t km^{-2} a^{-1})	Relative error (%)[a]	Trap efficiency	Source
1968–1984					
5.90×10^6	347,000	8100	6.4	0.65	Griffiths and McSaveney (1986)
		12,500		0.65	Griffiths and McSaveney (1986)
1982–1992					
1.90×10^6	201,000	4700	8.0		This Study
		7200		0.65	Griffiths and McSaveney (1986)
		12,400		0.38	This Study
1992–2001					
2.45×10^6	263,000	6200	10.0		This Study
		9500		0.65	Griffiths and McSaveney (1986)
		12,600		0.49	This Study
1968–2001					
1.03×10^7	289,000	6800	30.0		This Study
		10,400		0.65	Griffiths and McSaveney (1986)
		11,500		0.59	This Study
		12,500		0.54	Average (1968–2001)

Bold figures are corrected for respective values of trap efficiency.
[a] Mean relative error, i.e., maximum deviation divided by the mean.

these required parameters have been resampled. Interestingly, the lower Waitangitaona River appears to have had an increase in overall stream competence, favouring the transport of particle diameters <80 mm (b axis) to the delta front as opposed to earlier measurements of <5 mm (Griffiths and McSaveney, 1986). Applying these corrections and the new survey data, the existing record of specific sediment yield has been extended substantially (Table 1). Averaged rates for several sampling periods range between 7200 and 12,600 t km^{-2} a^{-1} and correspond well with earlier data (Griffiths and McSaveney, 1986). The accuracy of these figures however is largely a function of the calculated trapping efficiency. The averaged sediment yield for the period of 1968–1984 was inferred to be 12,500 t km^{-2} a^{-1}, based on a trapping efficiency $E_t = 0.65$ on the terminal fan (Griffiths and McSaveney, 1986). Main-

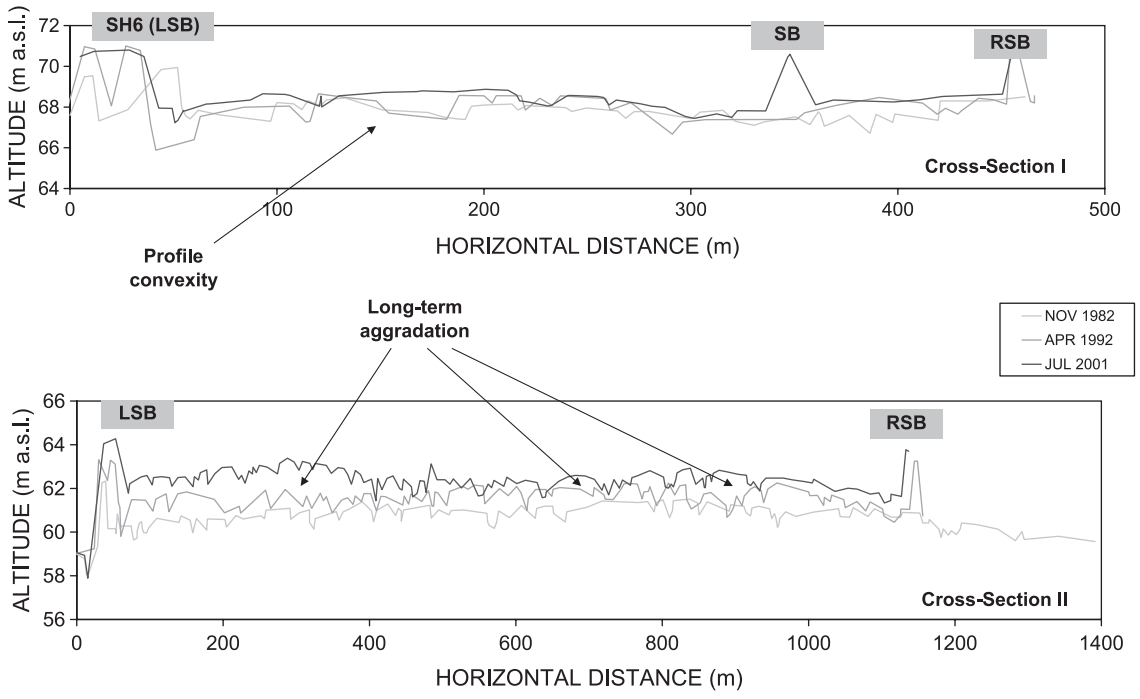

Fig. 10. Selected multitemporal cross-sections on the Waitangitaona River terminal fan downstream of State Highway 6 (SH6) bridge; left stopbank (LSB); right stopbank (RSB); additional stopbank (SB). Note the overall cross-sectional convexity of the outwash fan and the long-term trend of aggradation, which has led to an average superelevation of ~ 2 m above the SH6 level (origin of *x*-axis in cross-section 2, at ~ 59 m a.s.l.).

tenance of this yield for the period of 1982–1992 would require a decrease to $E_t = 0.38$, which accords to the observations made at the present delta head (Table 1).

The variation in these rates illustrates the need for long-term surveys of sediment movement in large gravel-bed rivers. Comparison of the yield on the terminal fan with that inferred at Gaunt Creek confluence also suggests net sediment retention of <50% on the active braidplain between Gaunt Creek and SH6 (LW, Fig. 8). Although this reach offers little conclusive morphologic evidence of former aggradation pulses, scour marks on several exhumed in situ tree stumps on the true left hint at historic braidplain accretion with minimum burial depths of ~ 1.8 m, approximately 500 m upstream of SH6. Assuming a conservative average value of 1 m of post-1948 aggradation in this reach, temporary sediment storage would amount to ~ 2×10^6 m^3.

5. Discussion

All three recent large landslides presented above have left distinctive long-range geomorphic impacts in their respective river catchments. These off-site effects of channel or valley floor burial, and subsequent river avulsion or metamorphosis may extend up to 10 km from the initial failure site. They have invariably resulted from massive input of landslide debris into the fluvial system by means of various delivery modes (Table 2).

Average short-term rates of erosion of landslide debris range from nearly 0.1 to 2.5×10^6 m^3 a^{-1}. Major problems, however, arise with the quantification of such disturbance, particularly when attempts are made to distinguish or isolate the landslide-derived sediment from the upstream or "background" yield. Values should be treated with care as they have been approximated from a DEM. Water content and bulk density (assumed to be

Table 2
Summary of landslide characteristics and geomorphic impact on alpine river systems for the examples presented

	Falling Mountain, Otehake River	Mt. Adams, Poerua River	Gaunt Creek, Waitangitaona River
Physiographic setting	Alpine headwaters (Main Divide)	V-shaped alpine valleyside wall	Mountain front-range failure
Landslide source location	Openslope	Ridge crest	Ridge crest/openslope
Lithology of source rock	Fractured greywacke, argillite	Fractured schist, colluvium	Cataclasite, mylonite schist
Type of landslide/slope failure	Rock avalanche	Rock avalanche	Complex gully/slip system
Scale of duration of slope instability	1–2 min	Several minutes	Several decades (most of 20th century)
Date of failure	1929	1999	1918[a]
Trigger	Earthquake	None known	Landslide-induced fluvial undercutting (inferred)
Landslide Volume (10^6 m^3)	55	10–15	>7.7
Apparent erosion rate of debris (m^3 a^{-1})	151,400	140,000–2,500,000	99,500–368,800
Apparent sediment yield (t km^{-2} a^{-1})	35,200 ± 2300	75,700 ± 4600[b]	26,800[c]
Length of directly impacted channel (km)	4.5	1.4	0.9
Range of major off-site impact (km)	unknown	>7.5	9.5
Delivery mode	Axial	Lateral	Coupled fan–trunk fan system
Dominant landslide impact	Complete obliteration and burial of headwater reaches, minor landslide ponds	Temporary landslide dam (Type III after Costa and Schuster, 1988), massive postfailure downstream aggradation	Massive downstream aggradation on alluvial tributary fan and trunk channels
Type of fluvial response	Reexcavation of headwater channel by establishment of retrogressive spring seepage canyons in highly disrupted landslide debris	Rapid reworking of landslide debris, temporary intramontane and mountain fringe fanhead storage, major downstream avulsion	Massive downstream aggradation, large-scale trunk channel avulsion on mountain fringe fanhead

Bold figures indicate averages over the total respective observation period.
[a] First historical records.
[b] Short-term yield (27 months).
[c] Gaunt Creek confluence.

1.8 t m^{-3}) of sediment, and percentage of suspended load may vary significantly and thus alter the figures of specific sediment yield by as much as ± 30%. Moreover, in the specific case of Westland rivers, data on ''background'' sediment flux are limited by the fact that the present temporal observation window may be shorter than the recurrence interval for major disturbances, and thus be characterised by pulses rather than long-term averages.

The estimated sediment yield from the Falling Mountain event is the highest for rock avalanche derived sources in the Southern Alps (cf. Whitehouse, 1983) and probably most closely represents exclusive landslide-derived supply rates. Both its situation in an alpine headwater catchment and dominant drainage by seepage-fed streams emerging from within the landslide deposit eliminate upstream or tributary yield, resulting in a discharge rate of ~150,000 m^3 a^{-1} (Table 3). Generally, discharge rates vary by one order of magnitude between 10^5 and 10^6 m^3 a^{-1}.

The exceedingly high apparent delivery rate following the Mt. Adams rock avalanche is about twice the amount of suspended sediment yield reported from several alpine Westland catchments (Griffiths, 1979; Hicks et al., 1996), but leaves unaccounted for amounts of sediment input from upstream sources. The trend of time-averaged de-

Table 3
Apparent net sediment delivery from the three example catchments affected by large landslides

Location		Net Balance			
Period	Years	Contributing catchment area (km^2)	Sediment volume input (m^3)	Sediment volume output (m^3)	Apparent sediment discharge[a] ($m^3\ a^{-1}$)
Poerua (alluvial fan)					
May 99–Nov 99	0.5	59	932,800		1,865,600
Nov 99–Jun 00	0.6	59	342,700		587,500
Jun 00–Dec 00	0.5	59	165,500		330,900
Dec 00–Feb 02	1.2	59	163,400		140,100
May 99–Feb 02	2.8	59	**1,699,000**		**617,800**
Poerua (lower gorges)					
Oct 99–Jan 02	2.3	51	**5,683,400**		**2,525,900**
Gaunt Creek fan					
1918–1965	47.0	9	**7,700,000**		**163,800**
1965–2001	36.0	9		**3,582,700**	**99,500**
Waitangitaona terminal fan					
1968–1984	16.0	74	5,900,000		368,800
1982–1992	10.0	74	1,895,900		189,600
1992–2001	9.0	74	2,445,100		271,700
1968–2001	33.0	74	**10,329,700**		**313,000**
Falling Mountain					
1929–1991	62.0	8		**9,387,100**	**151,400**

Bold figures denote totals over the respective observation periods.
[a] Not corrected for trap efficiency.

crease of the apparent delivery rate of sediment to the Poerua fanhead may be roughly exponential (Fig. 11). This trend must be treated with caution because the rate does not include the sediment flux through the newly established avulsion channel, which has only been surveyed as of 2002; the former course of the Poerua has largely been abandoned. Despite the incipient aggradation pulse in the former channel, the average bed slope has remained somewhat constant since June 2000, possibly indicating the onset of avulsion (Table 4). The average slope of the avulsion channel is smaller than that of the former course. This is due to effects of ongoing aggradation, which have not been recorded in earlier surveys.

In any case, the amount of landslide-induced sediment conveyance is significant even for alpine catchments (e.g., Anthony and Julian, 1999). In the Gaunt Creek example, where material supplied from chronic or continuous slope failure at Gaunt Creek Slip has arguably caused decadal-scale overloading of the lower Waitangitaona River, pinpointing the relevance of landslide debris input is probably most difficult. Although deposition of sediment in the terminal fan-building process has been most pronounced following the 1967 avulsion event, the gradual decline was interrupted by another period of net material accumulation in the 1990s with apparent delivery rates of almost 75% of those of the postdisturbance interval (Table 3). Correspondingly, the specific sediment yield following the avulsion event appears not to be markedly higher than those of the following decades (Table 1). Surely, the accurate calculation of sediment trapping efficiency is a crucial source of error in data processing.

Obviously, the natural variability as evident in the complex response of fluvial systems to overloading poses substantial difficulties in isolating single disturbances or sediment sources. We further-

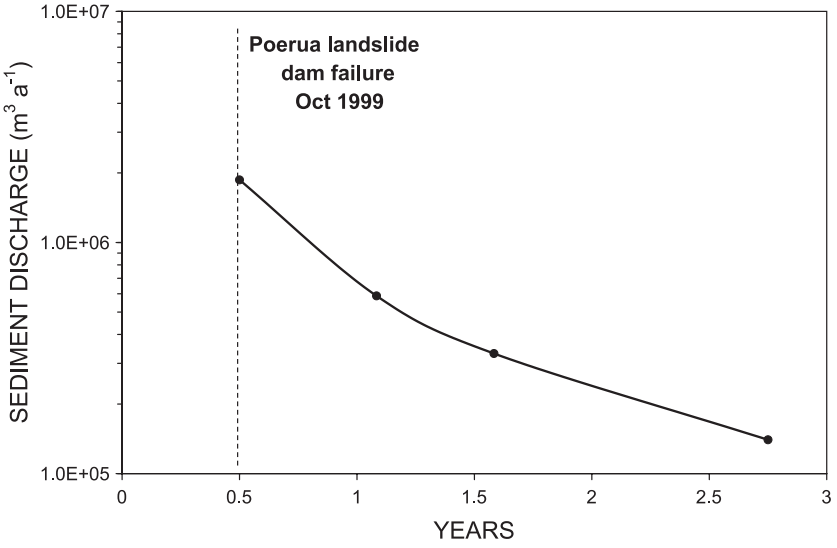

Fig. 11. Time-dependent decline of net sediment input rates on the upper Poerua River alluvial fan. The average net sediment discharge following landslide dam failure amounted up to nearly 2×10^6 m^3 a^{-1}. Rates were derived from cross-sectional surveys (Fig. 7, Table 3).

more suspect that traditional models of floodplain dynamics do not apply to the Poerua and Waitangitaona River valley floors. It seems that these valley floors become inundated only after exceptional sediment inputs; thus, the rivers remain incised into their deposits during undisturbed conditions. The valley floors are aggrading episodically after landslide dam break events, earthquakes, or chronic slope instability, while the rivers are normally at grade at a lower slope and elevation to which they return after each aggradation episode. This may apply to many other Westland rivers, which have recent "floodplain" and fan soils, but are presently incised by several metres. This simple model of episodic high-magnitude aggradation and postevent incision underlines but one of the problems associated with accurately determining sediment volumes and flux in alpine river systems.

Table 4
Average channel bed gradients for upper Poerua alluvial fan at the avulsion site

	Former channel	Avulsion channel
May-99	0.0136	–
Nov-99	0.0145	–
Jun-00	0.0150	–
Dec-00	0.0151	–
Feb-02	0.0151	0.0122

6. Conclusions

Large (>10^6 m^3) landslides are important major sources of sediment in alpine rivers. Excessive input of debris from such slope failures may form landslide dams and cause transport limitations. In the case of stable landslide dams, the deposition of large amounts of debris on the valley floors imposes a regulatory retention or buffering effect on reach-scale sediment flux, and initiates extensive backwater aggradation. In the western Southern Alps however, the entrainment and downstream routing of landslide debris more often causes catastrophic overloading of river channels, resulting in channel metamorphosis and avulsions on unconfined alluvial fans (Korup, 2003). Both scenarios have significant implications for developing models of river response in terms of sediment yield following either discrete slope failures or rainfall- or earthquake-triggered landsliding episodes (Beschta, 1983; Pearce and Watson, 1986). The three historic case studies display extreme short- to medium-term

sediment yields and provide a good benchmark on potential maximum fluvial sediment transport. They also complement previous studies on sediment discharge from dominantly smaller failures (e.g., Hovius et al., 1997; Martin et al., 2002). Despite the ongoing detection of large landslides in the Southern Alps, the lack of absolute age controls precludes their use for similar studies of landslide sediment supply, entrainment rates, consequential river response, or geomorphic hazard from such events. The large-scale avulsion of the Waitangitaona River highlights the potential for future similar events. It also underlines the geomorphic off-site hazards to settlements and infrastructure situated on unconfined alluvial fans of frequently landslide-affected alpine rivers.

Acknowledgements

We thank Mike Shearer, West Coast Regional Council, Greymouth, for supplying survey data on the Waitangitaona River. Dawn Chambers, Institute for Geological and Nuclear Sciences, Lower Hutt, kindly provided a recalculated radiocarbon age. We express our gratitude to Lincoln University for funding topographical surveys and aerial photography on the Poerua River as well as Geoff Kerr for survey data processing, and Ariane Walz for fieldwork support. Careful reviews by Robert Allison, Takashi Oguchi, and Mauro Soldati helped to improve an earlier manuscript.

References

Alvera, B., García-Ruiz, J.M., 2000. Variability of sediment yield from a high mountain catchment, Central Spanish Pyrenees. Arctic, Antarctic, and Alpine Research 32, 478–484.

Anthony, E.J., Julian, M., 1999. Source-to-sink sediment transfers, environmental engineering and hazard mitigation in the steep Var River catchment, French Riviera, southeastern France. Geomorphology 31, 337–354.

Beschta, R.L., 1983. Channel changes following storm-induced hillslope erosion in the Upper Kowai Basin, Torlesse Range, New Zealand. Journal of Hydrology. New Zealand 22, 93–111.

Carson, M.A., Griffiths, G.A., 1987. Bedload transport in gravel channels. Journal of Hydrology. New Zealand 26, 1–151.

Costa, J.E., Schuster, R.L., 1988. The formation and failure of natural dams. Geological Society of America Bulletin 100, 1054–1068.

Crosta, G.B., 2001. Failure and flow development of a complex slide: the 1993 Sesa landslide. Engineering Geology 59, 173–199.

Cruden, D.M., Varnes, D.J., 1996. Landslide types and processes. In: Turner, A.K., Schuster, R.L. (Eds.), Landslides, Investigation and Mitigation. Special Report, vol. 247. Transportation Research Board, National Research Council, Washington, DC, pp. 36–75.

Davies, T.R., McSaveney, M.J., 2000. Anthropogenic fanhead aggradation, Waiho River, Westland, New Zealand. In: Mosley, M.P. (Ed.), Gravel-bed Rivers V. Proceedings of Gravel-Bed Rivers 2000, 27 August–2 September 2000, Water Resources Publications, LLC, Christchurch, pp. 531–553.

Evans, M., 1997. Temporal and spatial representativeness of alpine sediment yields: Cascade Mountains, British Columbia. Earth Surface Processes and Landforms 22, 287–295.

Evans, M., Church, M., 2000. A method for error analysis of sediment yields derived from estimates of lacustrine sediment accumulation. Earth Surface Processes and Landforms 25, 1257–1267.

Fort, M., 1987. Sporadic morphogenesis in a continental subduction setting: an example from the Annapurna Range, Nepal Himalaya. Zeitschrift für Geomorphologie. Supplementband N.F. 63, 9–36.

Griffiths, G.A., 1979. High (suspended) sediment yields from major rivers of the Western Southern Alps, New Zealand. Nature 282, 61–63.

Griffiths, G.A., McSaveney, M.J., 1986. Sedimentation and river containment on Waitangitaona alluvial fan—South Westland, New Zealand. Zeitschrift für Geomorphologie 30, 215–230.

Hamblett, S., 1968. Waitangi-taona River Report. Water and Soil Division, Ministry of Works and Development, Christchurch. 16 pp.

Hancox, G.T., McSaveney, M.J., Davies, T.R., Hodgson, K., 1999. Mt. Adams rock avalanche of 6 October 1999 and subsequent formation and breaching of a large landslide dam in Poerua River, Westland, New Zealand. Institute of Geological and Nuclear Sciences Report, vol. 99/19. IGNS (Institute of Geological and Nuclear Sciences), Lower Hutt: 22 pp.

Henderson, R.D., Thompson, S.M., 1999. Extreme rainfalls in the Southern Alps of New Zealand. Journal of Hydrology. New Zealand 38, 309–330.

Hewitt, K., 1999. Quaternary moraines vs. catastrophic rock avalanches in the Karakoram Himalaya, Northern Pakistan. Quaternary Research 51, 220–237.

Hicks, D.M., McSaveney, M.J., Chinn, T.J.H., 1990. Sedimentation in proglacial Ivory Lake, Southern Alps, New Zealand. Arctic and Alpine Research 22, 26–42.

Hicks, D.M., Hill, J., Shankar, U., 1996. Variation of suspended sediment yields around New Zealand: the relative importance of rainfall and geology. In: Walling, D.E., Webb, B.W. (Eds.), Erosion and Sediment Yield: Global and Regional Perspectives. IAHS Publication, vol. 236, pp. 149–156.

Hovius, N., Stark, C.P., Allen, P.A., 1997. Sediment flux from a mountain belt derived from landslide mapping. Geology 25, 231–234.

Hovius, N., Stark, C.P., Chu, H.T., Lin, J.C., 2000. Supply and

removal of sediment in a landslide-dominated mountain belt: Central Range, Taiwan. Journal of Geology 108, 73–89.

King, J., Loveday, I., Schuster, R.L., 1989. The 1985 Bairaman landslide dam and resulting debris flow, Papua New Guinea. Quarterly Journal of Engineering Geology 22, 257–270.

Korup, O., 2003. Landslide-induced river disruption—Geomorphic imprints and scaling effects in alpine catchments of South Westland and Fiordland, New Zealand. Unpubl. PhD thesis. Victoria University of Wellington. 314 pp.

Korup, O., Crozier, M., 2002. Landslide types and geomorphic impact on river channels, Southern Alps, New Zealand. In: Rybar, J., Stemberk, J., Wagner, P. (Eds.), Landslides. Proceedings 1st European Conference on Landslides 24–26 June 2002, Prague. Balkema, Rotterdam, pp. 233–238.

Land Information New Zealand, 2000. 25-m Digital Elevation Model based on NZMS260 digital 20-m contours (scale 1:50,000). Published by Land Information New Zealand, Lambton Quay, Wellington. Crown Copyright reserved.

Martin, Y., Rood, K., Schwab, J.W., Church, M., 2002. Sediment transfer by shallow landsliding in the Queen Charlotte Islands, British Columbia. Canadian Journal of Earth Sciences 39, 189–205.

McSaveney, M.J., Davies, T.R., Hodgson, K.A., 2000. A contrast in deposit style and process between large and small rock avalanches. In: Bromhead, E., Dixon, N., Ibsen, M.L. (Eds.), Landslides in Research, Theory and Practice. Proceedings 8th International Symposium on Landslides 26–30 June, Thomas Telford, Cardiff, pp. 1052–1058.

Miller, D.J., Benda, L.E., 2000. Effects of punctuated sediment supply on valley-floor landforms and sediment transport. Geological Society of America Bulletin 112, 1814–1824.

Norris, R.J., Cooper, A.F., 2000. Late Quaternary slip rates and slip partitioning on the Alpine Fault, New Zealand. Journal of Structural Geology 23, 507–520.

Ohmori, H., 1992. Dynamics and erosion rate of the river running on a thick deposit supplied by a large landslide. Zeitschrift für Geomorphologie 36, 129–140.

Pearce, A.J., Watson, A.J., 1986. Effects of earthquake-induced landslides on sediment budget and transport over a 50-yr period. Geology 14, 52–55.

Ries, J.B., 2000. The landslide in the Surma Khola Valley, High Mountain Region of the Central Himalaya in Nepal. Physics and Chemistry of the Earth: Part B. Hydrology, Oceans and Atmosphere 25, 51–57.

Schiefer, E., Slaymaker, O., Klinkenberg, B., 2001. Physiographically controlled allometry of specific sediment yield in the Canadian Cordillera: a lake sediment-based approach. Geografiska Annaler 83A, 55–65.

Schuster, R.L., 2000. Outburst debris flows from failure of natural dams. In: Wieczorek, G.F., Naeser, N.D. (Eds.), Debris-flow Hazards Mitigation: Mechanics, Prediction, and Assessment. Proceedings 2nd International Conference on Debris Flow Hazard Mitigation, 16–20 August, Taipeh Balkema, Rotterdam, pp. 29–42.

Selby, M.J., 1988. Landforms and denudation of the High Himalaya of Nepal: results of continental collision. Zeitschrift für Geomorphologie. Supplementband N.F. 69, 133–152.

Selby, M.J., 1993. Hillslope Materials and Processes, 2nd edition. Oxford Univ. Press, Oxford. 280 pp.

Suggate, R.P., 1990. Late Pliocene and Quaternary glaciations of New Zealand. Quaternary Science Reviews 9, 175–197.

Sutherland, D.G., Ball, M.H., Hilton, S.J., Lisle, T.E., 2002. Evolution of a landslide-induced sediment wave in the Navarro River, California. Geological Society of America Bulletin 114, 1036–1048.

Walling, D.E., Webb, B.W. (Eds.), 1996. Erosion and Sediment Yield: Global and Regional Perspectives. IAHS Publication, vol. 236. 586 pp.

Whitehouse, I.E., 1983. Distribution of large rock avalanche deposits in the central Southern Alps, New Zealand. New Zealand Journal of Geology and Geophysics 26, 272–279.

Whitehouse, I.E., 1988. Geomorphology of the central Southern Alps, New Zealand: the interaction of plate collision and atmospheric circulation. Zeitschrift für Geomorphologie. Supplementband N.F. 69, 105–116.